

# Hedgehog Signaling in Human Medullary Thyroid Carcinoma: A Novel Signaling Pathway

Brittany Bohinc,<sup>1</sup> Gregory Michelotti,<sup>2</sup> and Anna Mae Diehl<sup>2</sup>

**Background:** Locally or widely metastatic medullary thyroid carcinoma (MTC) is difficult to treat, and therapeutic options are limited. Recently, kinase inhibitors have shown partial efficacy in this cancer, but there is a continued need for the development of novel therapeutics. Within this context, the Hedgehog (Hh) pathway has been implicated in several types of human tumors, and early clinical trials with Hh antagonists have validated Hh as a novel therapeutic target. For the first time, we evaluated Hh pathway activity in MTC, and examined the effect of Hh pathway perturbation in highly characterized MTC cell lines.

**Methods:** We examined immunohistochemical expression of the Hh signaling mediators Sonic Hedgehog (Shh) and Glioblastoma (Gli)2 in paraffin-embedded normal versus histologically characterized human MTC tissue. We examined pharmacologic disruption of Hh signaling *in vitro* using two established MTC cell lines (TT and MZ-CRC-1). Hh signaling was either pharmacologically activated (SAG) or inhibited (GDC-0449) in MTC cell lines; Hh activity was assessed by quantitative real-time polymerase chain reaction, Western blot analysis, and quantification of cellular growth and apoptotic activity.

**Results:** Our data showed increased expression of Hh signaling factors in human MTC compared to normal tissue. *In vitro*, activation of the Hh pathway resulted in increased expression of key Hh signaling components Smoothed (Smo) and Gli2. Conversely, inhibition of the Hh pathway decreased expression of these genes, leading to significantly reduced cellular growth and increased apoptosis.

**Conclusions:** Hedgehog signaling components are markedly upregulated in MTC. Hh pathway inhibitors have potential as novel therapeutic options in patients with metastatic and/or surgically unresectable MTC.

## Introduction

MEDULLARY THYROID CARCINOMA (MTC) occurs at an estimated prevalence of 0.14% in the general population, but affects nearly all patients with multiple endocrine neoplasia (MEN) type 2 syndromes (1,2). Cumulatively, MTC accounts for 5–10% of all thyroid cancer. Despite a relatively low population prevalence, MTC is responsible for a disproportionate amount of thyroid cancer deaths at 13.4% (3). Although associated with a favorable prognosis when surgical resection is curative, MTC is not easily treated when it has metastasized beyond the thyroid bed. New therapies (e.g., vandetanib and cabozantinib) have focused on tyrosine kinase (TK) receptors and the vascular endothelial growth factor (VEGF) receptor as potential therapeutic targets in advanced metastatic disease. Unfortunately, these drugs have multiple side effects, a difficult tolerability profile, and have no effect on mortality. Therefore, it is important to continue to explore new cellular signaling pathways in MTC and pursue novel therapeutic approaches.

MTC is derived from parafollicular C cells, which are derived from ectodermal neural crest cells located in the endodermally derived fourth pharyngeal pouch and ultimobranchial body. Various embryologic signaling pathways have been noted to play a role in ectodermal tissue repair, regeneration, and tumor growth. Hedgehog (Hh) is a morphogenic signaling pathway described as being involved in the development of multiple endodermal and ectodermally derived tissues (4–6). It is activated by a family of Hh-specific ligands—Sonic Hedgehog (Shh), Indian Hedgehog (Ihh), and Desert Hedgehog (Dhh)—that bind to their receptor, Patched (Ptc). Ptc resides on the surface of Hh-responsive target cells and tonically inhibits Smoothed (Smo), the Hh signaling receptor component. Binding of the Hh ligand to Ptc causes the release of inhibitory actions of Ptc on Smo, leading to Smo activation, which, in turn, results in the stabilization and nuclear localization of Gli family transcription factors (Gli1, Gli2, Gli3). The Glis then control the expression of Hh-regulated genes (Fig. 1). Hence, nuclear accumulation of Gli is the endpoint of the canonical Hh signaling pathway. Hh

<sup>1</sup>Division of Endocrinology, Diabetes, and Metabolism; <sup>2</sup>Division of Gastroenterology; Duke University Medical Center, Durham, North Carolina.

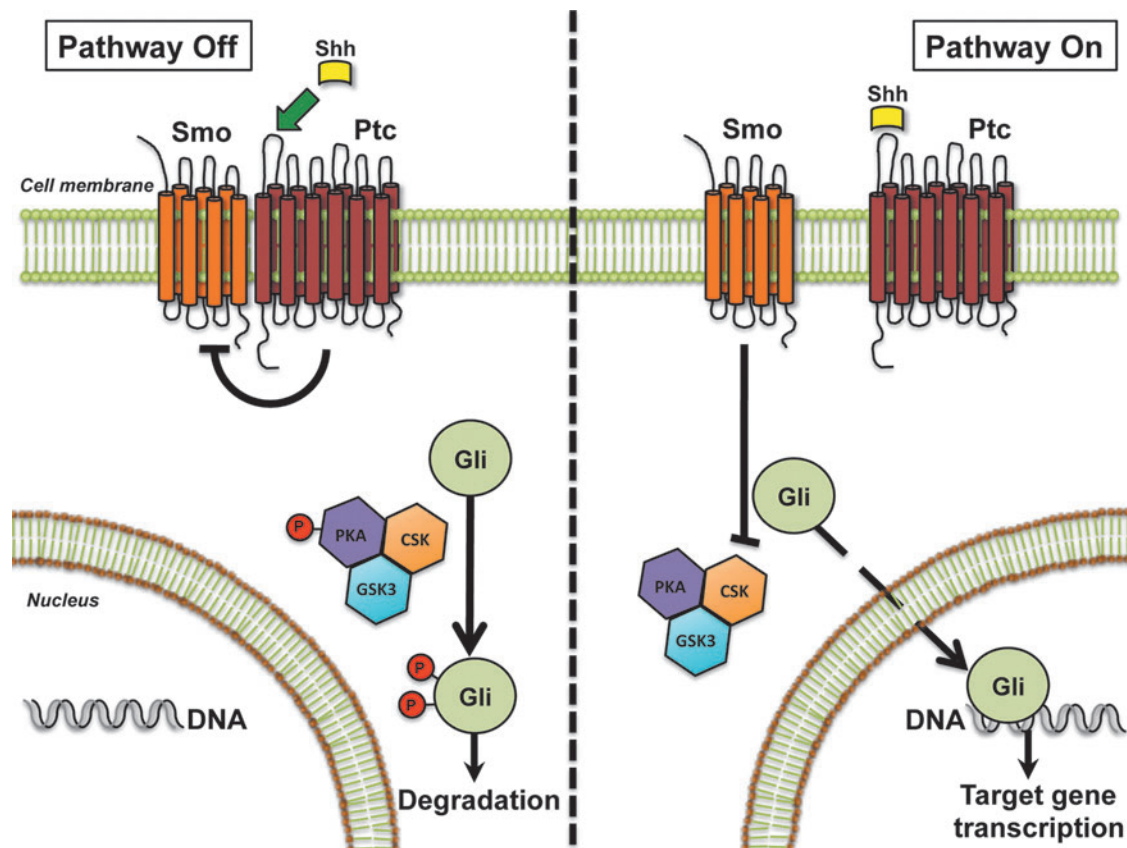


**FIG. 1.** Hedgehog signaling pathway, a morphogenic signaling pathway important in embryogenesis, tissue differentiation, cell growth and development. In adults, it is upregulated in certain injured tissues and in certain types of cancer. The Sonic Hedgehog ligand (i.e., Shh) binds to its receptor, Patched (Ptc), which, in turn, derepresses Smoothed (Smo), another transmembrane receptor in a chronically inactive state. Activation of Smo drives downstream Hh signaling, causing nuclear accumulation of Glioma-associated factors 1, 2, and 3 (Gli1, Gli2, Gli3) and transcription of Hh target genes. *Illustration by Steve Choi, MD.*

signaling is critical in cellular proliferation, apoptosis, migration, differentiation, and the growth of progenitor cell populations. Although largely quiescent in adult tissues, it is aberrantly upregulated in injured tissue (i.e., liver fibrosis and tissue injury) and in some forms of tumorigenesis. Thus, we wished to determine if Hh signaling is present in human MTC and if inhibition of the cellular signaling pathway would have tumoricidal effects and clinical utility in patients with advanced disease.

## Materials and Methods

### *Immunohistochemical staining for calcitonin, Shh, and Gli2*

Normal human thyroid tissue and seven human MTCs were obtained from the institutional review board (IRB)-approved Duke Department of Pathology at Duke University Medical Center. Paraffin-embedded tissue was sectioned, treated with Xylene, and rehydrated. Antigen retrieval was performed after heating tissue in 10 mM sodium citrate buffer for 10 minutes. Sections were blocked with Dako solution (Dako Envision). Primary antibodies for calcitonin (1:1500; Dako polyclonal rabbit antihuman antibody), Gli2 (1:2000; GenWay Biotech, Inc. Kruppel family member GLI2 (Gli2) rabbit antihuman polyclonal (aa 46–60) antibody), and Shh

(1:1000; GenWay Biotech, Inc., polyclonal anti-SHH antibody) were added to tissue sections and incubated overnight at 4°C. Secondary antirabbit antibodies were added the next day, and the tissue was treated for one hour at room temperature. Stains for Shh and Gli2 protein expression were developed using 3,3'-Diaminobenzamine (DAB) developing solution (DAB Substrate Chromogen System, Dako, K3466) and counterstained for hematoxylin and eosin (H&E) per standard protocol. Slides were fixed with xylene mount, and images were obtained with an Olympus IX71 inverted microscope using the DP2-BSW (Olympus) image acquisition software system. Quantification of calcitonin-positive tumor cells staining for SHH and/or Gli2 was obtained by cell count in 10 representative fields of view at 40× magnification and reported as mean ± standard deviation.

### *Human medullary cell lines*

Two cell lines were used in this experiment. The TT human MTC cell line (ATCC) and the MZ-CRC-1 human MTC cell line (kindly provided by Dr. Robert Gagel at the MD Anderson Cancer Center) were utilized (7,8). The TT cell line was derived from a patient with MEN2A carrying a heterozygous C634W RET mutation. The MZ-CRC-1 cells were derived from a patient with MEN2B and the M918T mutation. TT Cells were grown in Ham's F12K media (Sigma-Aldrich)

containing 10% fetal bovine serum (Gibco) and 1% penicillin/streptomycin (10,000 units penicillin and 10 mg streptomycin per mL in 0.9% NaCl; Sigma-Aldrich). MZ-CRC-1 cell lines were grown in Dulbecco's modified Eagle's medium (DMEM) 1× high glucose (Sigma-Aldrich) containing 10% fetal bovine serum (Life Technologies, Inc.) and 1% penicillin/streptomycin (10,000 units penicillin and 10 mg streptomycin per mL in 0.9% NaCl; Sigma Aldrich).

For manipulative cell experiments, 50,000 cells were plated per well on a standardized six-well plate. Cells were treated with SAG (Enzo Life Sciences), a highly potent Smo agonist, at 0  $\mu$ M (vehicle, dimethyl sulfoxide (DMSO); Sigma), 0.075  $\mu$ M, and 0.3  $\mu$ M concentrations, and harvested at 24, 48, and 72 hours in TRIzol solution (Life Technologies, Inc.). Additionally, cells were treated with GDC-0449 (Vismodegib, Selleck Bio), a Smo antagonist, at concentrations of 0  $\mu$ M (vehicle, DMSO), 2  $\mu$ M, and 10  $\mu$ M. Cells were also treated with the 0.4  $\mu$ M concentration of GDC-0449 when obtaining protein for Western blot analysis to examine the dose-dependent relationship between Gli2 protein expression and GDC treatment. All drug doses were consistent with published literature utilizing similar oncogenic cell lines (9).

#### Quantitative real-time polymerase chain reaction

Cellular RNA was isolated from individual cell lines with TRIzol solution (Life Technologies, Inc.) and quantified by Nanodrop 2000 (Thermo Scientific). Total RNA was extracted from cells, liver, or brain using TRIzol (Invitrogen), followed by RNase-free DNase I treatment (Qiagen). RNA was reverse transcribed to cDNA templates using random primer and superscript RNase H-reverse transcriptase (Invitrogen) and amplified.

For semiquantitative qRT-PCR, 1.5% of the first-strand reaction was amplified using the StepOne Plus Real-Time PCR platform (ABI/Life Technologies). qRT-PCR parameters were as follows: denaturation at 95°C for 3 minutes, followed by 40 cycles of denaturing at 95°C for 10 s, and annealing-extension at the optimal primer temperatures for 60 s. Threshold cycles ( $C_t$ ) were automatically calculated by the StepOne Plus Real-Time Detection System. Target gene levels were presented as fold-over control according to the  $2^{-\Delta\Delta C_t}$  method relative to expression of the human beta actin ( $\beta$ -actin) housekeeping gene. All tests were performed in sextuplicate. Primer sequences for human *Shh*, *Gli2*, and *Smo* were previously described by our group (10).

#### Western blot

Western blot was performed for Gli2 in TT cells treated with GDC at doses of 0  $\mu$ M, 0.4  $\mu$ M, 2  $\mu$ M, and 10  $\mu$ M. At the indicated time, cells were harvested, and TT cell lysates were generated using standard Laemmli buffer. Lysates were analyzed by SDS-PAGE (Criterion 4–20%; Bio-Rad) and transferred to polyvinylidene difluoride membranes (Bio-Rad). Membranes were blocked for one hour at room temperature with 5% nonfat dry milk in TBS-T (TBS/0.05% Tween 20) and incubated at 4°C overnight with antibodies specific for Gli2 (1:1000; GenWay Biotech, Inc., Kruppel family member GLI2 (Gli2) rabbit antihuman polyclonal (aa 46–60)) and human  $\beta$ -actin antibody (1:1000; GenWay Biotech, Inc., actin-beta antibody). Proteins were detected using a HRP-linked sec-

ondary antibody (1:20,000; Sigma-Aldrich) and ECL reagent (Pierce).

#### Cell viability assay

Cell number plotted over time was used as a surrogate test for cell growth and evaluated by Cell Counting Kit-8 (CCK-8; Dojindo Molecular Technologies). A total of 5,000 cells were plated per well in a 96-well plate, as per the manufacturer's instructions. Cells were treated with vehicle (DMSO), SAG 0.3  $\mu$ M, or GDC 10  $\mu$ M, and incubated in a humidified incubator at 37°C, 5% CO<sub>2</sub>. Absorbance measurements were made by the FluoroStar Optima plate reader (BMG Labtech) at excitation filter 465 nm. Cells were plated, treated, and measured in sextuplicate. Absorbance readings were obtained at 0, 24, 48, and 72 hours.

#### Measurement of apoptosis

Cell death was then measured by Apo-ONE<sup>®</sup> Homogenous Caspase-3/7 Assay (Promega) utilizing cells treated with vehicle and GDC 10  $\mu$ M. A total of 20,000 cells per well were plated on a 96-well plate, treated with Apo-ONE<sup>®</sup> Caspase-3/7 Reagent (composed of Caspase Substrate Z-DEVD-R110 (100X) and Apo-ONE<sup>®</sup> Homogeneous Caspase-3/7 Buffer) and either vehicle (DMSO) or GDC 10  $\mu$ M, and incubated at room temperature. Fluorescence was measured at an excitation wavelength of 485 nm and an emission wavelength of 520 nm. Measurements were made at 0, 12, 24, 28, 33, 42, 48, 51, and 72 hours and plotted against time.

#### Statistical analysis

Two-tailed Student's *t* tests were performed for all analyses utilizing JMP statistical software (V7.0; SAS Institute Inc.). Microsoft Excel for Mac 2011 chart navigator (V14.0.0) was used to produce boxplots and linear plots. Statistical significance was defined as  $p < 0.05$ .

## Results

Immunohistochemical (IHC) staining of normal, uninjured thyroid tissue for both Shh and Gli2 revealed no Hh activity (Fig. 2A). In contrast, Shh strongly stained in the cytoplasm of parafollicular cells in the MTCs. Gli2, a downstream target of Hh signaling, was also expressed in the nuclei of MTC cells (Fig. 2B). All seven tumors were positive for Hh by IHC. Hedgehog staining pattern varied among the seven MTC tumors examined, with some tumors staining intensely for both Shh and Gli2 and other staining for Shh, but minimally for Gli2. Percentage of positive cells were quantified per 40× high-powered field (hpF) and averaged over 10 representative tumor fields (Fig. 2C). Additional images of tumor staining patterns at lower intensity magnification (4×) are provided in Supplementary Figure S1 (Supplementary Data are available online at [www.liebert.com/thy](http://www.liebert.com/thy)).

Quantitative real-time PCR was performed on both TT cells and MZ-CRC-1 cell lines for Gli2 and for Smo, the cell surface receptor and target of drug manipulation. TT cells treated with SAG 0.075  $\mu$ M and 0.  $\mu$ M showed significantly increased expression of Gli2 mRNA by 24 hours compared with vehicle (DMSO) in a dose-dependent manner. Smoothed mRNA expression was also significantly upregulated by treatment with SAG after 48 hours (Fig. 3A and B). Conversely, TT cells

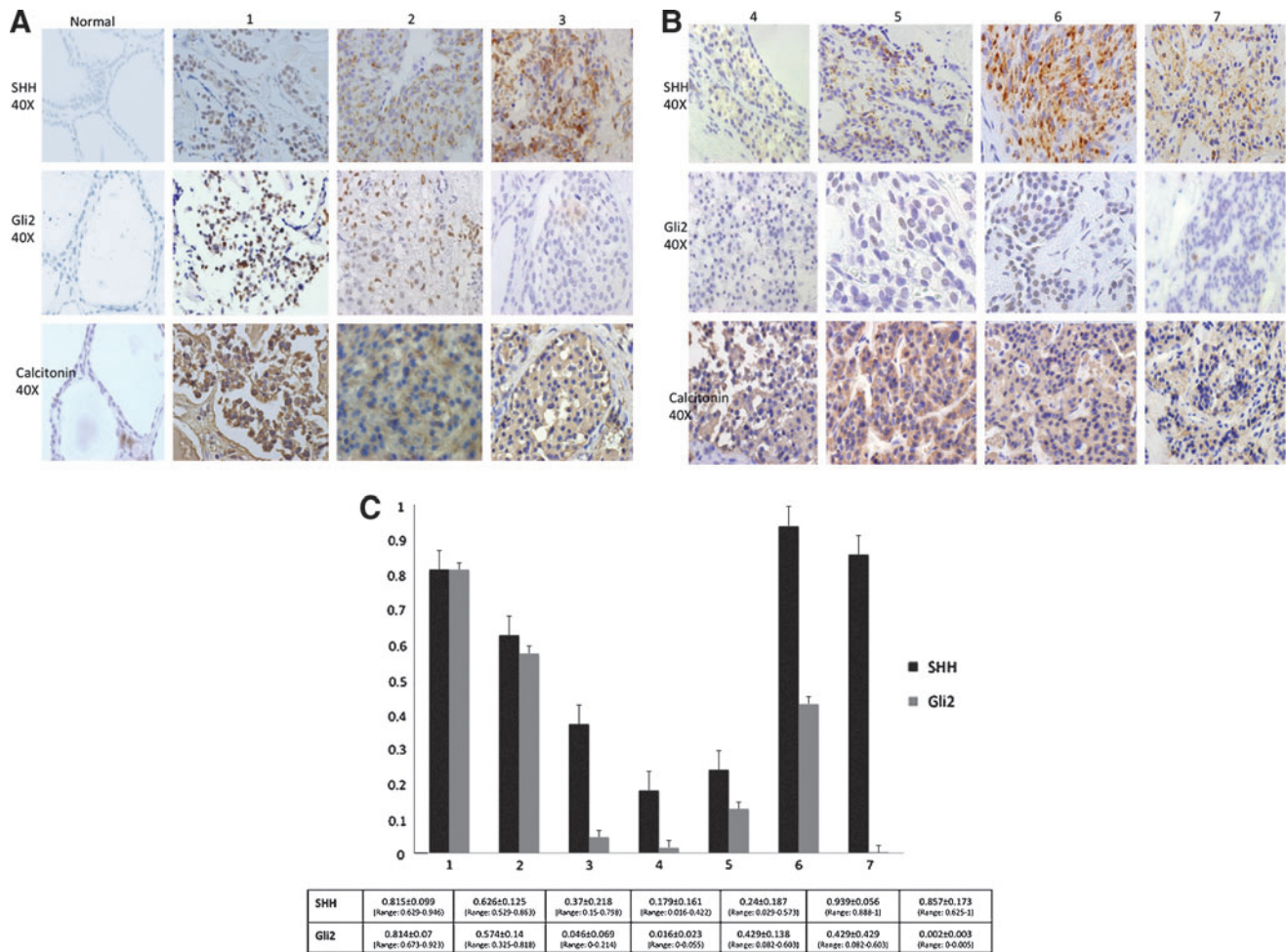


**FIG. 2.** (A) and (B) Expression of Shh and Gli2 is increased in medullary thyroid carcinoma (MTC) tissue. Representative immunohistochemistry from seven patients with biopsy-proven MTC shows significant expression of both cytoplasmic Shh and nuclear Gli2 in MTC but absence of Shh and Gli2 staining in normal thyroid tissue. Calcitonin staining is also shown to verify MTC and show presence of parafollicular cells in normal thyroid tissue; Normal tissue is classified as normal. MTC tumors are classified from 1 to 7. Magnification 40 $\times$ . (C) Graphical representation for all seven tumors showing the percentage of positive staining cells for Shh and Gli2 per 40 $\times$  high-powered field (hpF) averaged over 10 representative fields. Tumors are labelled from 1 to 7. Percentage positive cells for Shh and Gli2 is reported as a mean  $\pm$  standard deviation, and the range of positivity across the tumor is reported. Error bars are reported as standard error of the mean.

treated with GDC showed significant downregulation of *Gli2* and *Smo* by 24 and 48 hours respectively. Doses of GDC 2  $\mu$ M and 10  $\mu$ M were comparable in efficacy at reducing *Gli2* and *Smo* mRNA expression, although 10  $\mu$ M appears to have reduced *Gli2* expression to a greater degree within the first 24 hours of treatment (Fig. 3C and D). Similar reductions of mRNA expression in both *Gli2* and *Smo* were seen in the MZ-CRC-1 cell line after treatment with both GDC 2  $\mu$ M and 10  $\mu$ M compared with vehicle (DMSO; Supplementary Fig. S2).

Western blot was performed on TT cell lysates in Laemmli buffer. Clear bands were detected at 133 kD for *Gli2* (isoform a) and at 41 kD for human  $\beta$ -actin, consistent with published molecular weights (www.uniprotkb.com). A clear dose-dependent reduction in *Gli2* protein concentration was elucidated with highest concentrations of GDC-0449 having the greatest effect on protein suppression (Fig. 3C).

Cell viability assay (CCK-8) showed significantly increased cell number among TT cells treated with SAG, a *Smo* agonist,

at 0.3  $\mu$ M by 48 hours in culture (compared with placebo;  $p=0.023$ ). In addition, cell numbers had markedly declined by 48 hours in TT cells treated with GDC-0449, a *Smo* antagonist, at 10  $\mu$ M ( $p=0.002$ ). In addition, the slope of the line indicating cell proliferation was markedly decreased in the cell group treated with GDC (Fig. 4A). There was a treatment-related difference in the concentration of orange formazan dye, which marks viable cells, by direct visual examination of the 96-well plate among cells treated with SAG 0.3  $\mu$ M, vehicle, or GDC 10  $\mu$ M (Fig. 4B).

Because cell growth and number were markedly reduced by CCK-8 cell proliferation assay, we examined apoptotic activity in our TT cell culture model. Although differences in caspase-3 and -7 activity were noted between GDC 10  $\mu$ M and vehicle at 24 hours, significant differences in activity were not seen until 28 hours ( $p=0.002$ ). Caspase-3 and -7 activity remained significantly elevated in cells treated with GDC versus vehicle throughout the 72 hours of measurement (Fig. 5), indicating that abrogation of Hh signaling is sufficient to

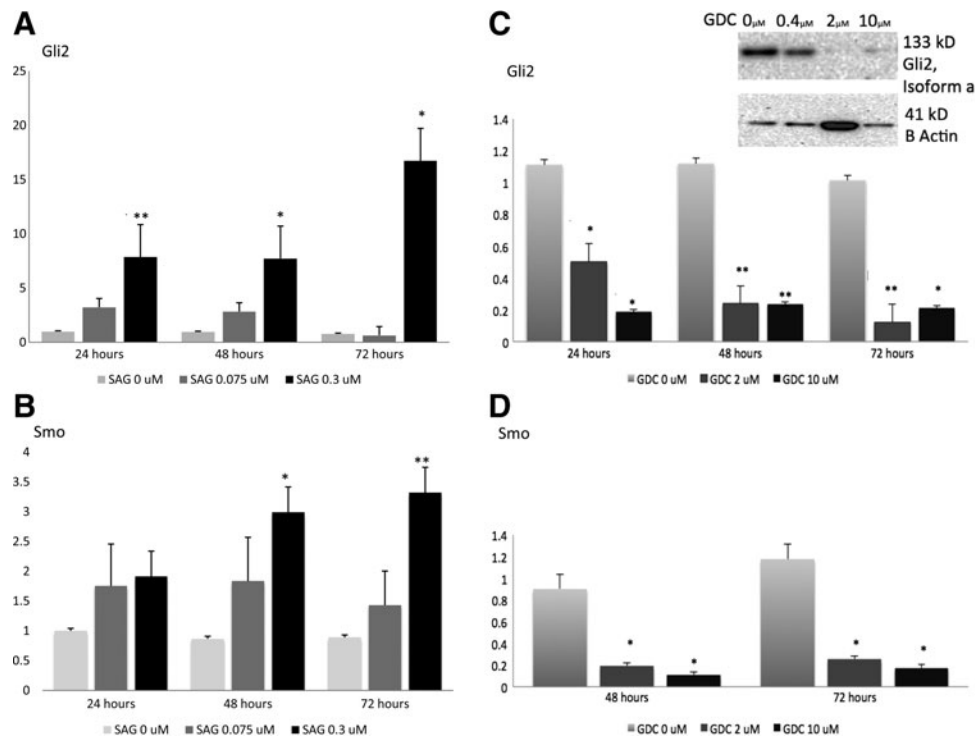


**FIG. 3.** Human MTC cells (TT) are Hh responsive. TT cells were grown in culture and treated with either SAG 0.075  $\mu$ M, SAG 0.3  $\mu$ M or vehicle control (DMSO), as described in the Materials and Methods. At the indicated time point, cells were harvested, RNA was isolated, and effects on *Gli2* (A) and *Smo* (B) gene expression were quantified by quantitative real-time polymerase chain reaction (qRT-PCR). (C) TT cells were treated with GDC 2  $\mu$ M or GDC 10  $\mu$ M versus vehicle control (DMSO) and *Gli2* mRNA expression levels were quantified by qRT-PCR. Cells showed a significant decrease in *Gli2* mRNA expression levels at both 2 and 10  $\mu$ M doses and at all time points. Inset shows representative Western blot for expression of Gli2 and the housekeeping protein,  $\beta$ -actin, in TT cells treated with GDC 0.4  $\mu$ M, 2  $\mu$ M, or 10  $\mu$ M versus vehicle control. (D) TT cells were treated with GDC or DMSO control at the indicated time point, as described above, and *Smo* mRNA expression levels were quantified by qRT-PCR. All statistical analyses were performed using a two-tailed Student's *t* test.  $p < 0.05$ \* were considered significant and  $p < 0.01$ \*\* highly significant.

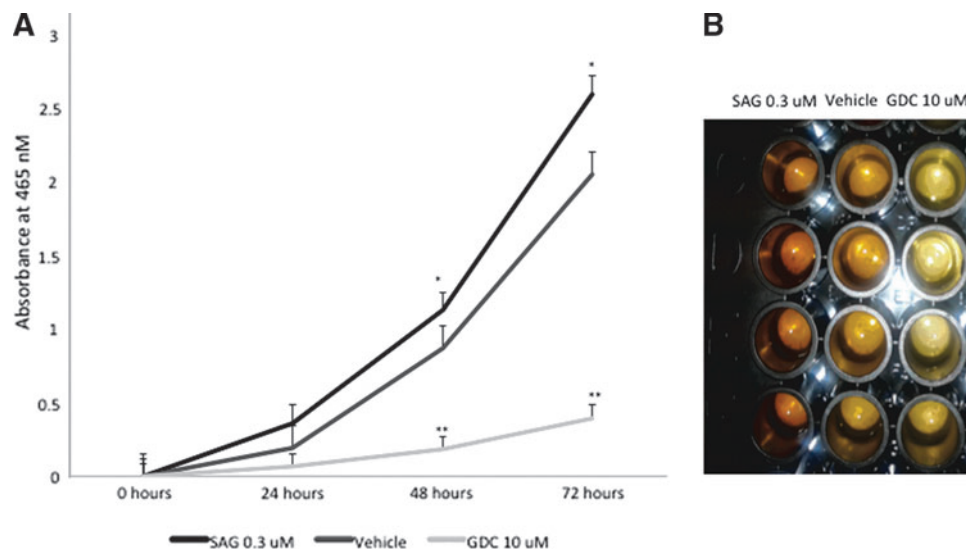


**FIG. 4.** Hh regulated human MTC cellular growth. (A) TT cells were plated in a 96-well plate at an initial cellular density of 5,000 cells/well. Cells were treated with vehicle (DMSO), SAG 0.3  $\mu$ M, or GDC 10  $\mu$ M and incubated in a humidified incubator at 37°C, 5% CO<sub>2</sub>. Absorbance readings were obtained at 0, 24, 48, and 72 hours as described in the Materials and Methods ( $*p < 0.05$  and  $**p < 0.01$ ). (B) The concentration of orange formazan dye is directly proportional to viable cells in samples treated with DMSO vehicle, SAG 0.3  $\mu$ M, or GDC 10  $\mu$ M. All statistical analyses were performed using a two-tailed Student's *t* test.  $p < 0.05$ \* were considered significant and  $p < 0.01$ \*\* highly significant.

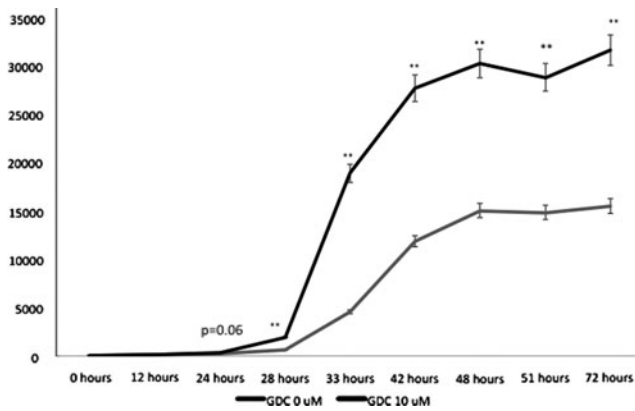


**FIG. 5.** Inhibition of Hh signaling causes apoptosis in human MTC cells. TT cells treated with DMSO vehicle (GDC 0  $\mu$ M) or GDC 10  $\mu$ M were plated at a density of 20,000 cells/well in a 96-well plate caspase-3 and -7 activity were measured at the indicated time points, as indicated in the Material and Methods. All statistical analyses were performed using a two-tailed Student's *t* test. \**p* < 0.05, significant; \*\**p* < 0.01, highly significant.

drive apoptosis in human MTC. Collectively, the data suggest that Hh pathway activity is necessary for MTC cellular viability and growth, and consistent with a role for Hh perturbation in cellular dysregulation.

## Discussion

MTC accounts for 5–10% of all thyroid cancers. Metastatic MTC is common, and treatment of metastatic tumor can be quite challenging. In fact, 35–50% of patients present with lymph-node involvement on initial diagnosis, whereas 10–15% present with distant metastases (11). The mainstay of treatment for these patients is extensive surgical resection of the primary tumor and long-term monitoring of calcitonin/CEA levels with surgical debulking when appropriate. Only very recently have systemic therapies targeting metastatic disease in these patients entered the treatment armamentarium.

Current targeted pathways for the development of novel therapeutics in MTC have focused primarily on inhibition of Rearranged during Transfection (RET), VEGF, and epidermal growth factor receptor (EGFR). RET overactivation results in downstream activation of RAS, phosphatidylinositol 3-kinase (PI3K) pathways, nuclear factor- $\kappa$ B (NF- $\kappa$ B), signal transducer and activator of transcription (STAT), and  $\beta$ -catenin. Once activated, RET transmits mitogenic, survival and motogenic signals (12,13). The VEGF receptors, on the other hand, are a family of growth factor receptors that stimulates angiogenesis, endothelial cell proliferation, migration, survival, and vascular permeability. EGFR is another tyrosine kinase receptor important in growth factor action on tumor proliferation and growth. The multikinase inhibitors, vandetanib and cabozantinib, with action against VEGFR-1, VEGFR-2, VEGFR-3, RET, and EGFR and c-Met and VEGFR-2 respectively, are currently the only FDA-approved treatments for metastatic MTC. A recent placebo-controlled prospective trial (NCT00410761) assigned 331 patients with locally advanced and metastatic disease to study drug versus placebo. Progression-free survival (PFS) favored vandetanib (HR 0.46,

[CI 0.31–0.69], *p* < 0.001) after a median follow-up of 24 months. Despite improved PFS with vandetanib (30.5 months vs. 19.3 months in the placebo arm), there was no improvement in overall survival after 24 months. In addition, the data were complicated by crossover of patients with progressive disease from the placebo arm to the treatment arm. Nevertheless, vandetanib was FDA approved for treatment of metastatic MTC in April 2011, and is the most clinically effective treatment for this subgroup to date. Unfortunately, vandetanib, like other tyrosine kinase inhibitors, has multiple side effects, including diarrhea (56% of patients), rash (45%), hypertension (32%), nausea (33%), and QTc prolongation (14%), leading to significant dose reduction and discontinuation of the drug in 28% of patients (14). In addition, pre-clinical studies with vandetanib showed that the activating RET mutation, V804M, which accounts for almost 20% of those with hereditary MTC, is resistant to vandetanib, suggesting a need for additional therapeutic options for this cancer (15,16). Palliative chemotherapeutic regimens have been reported in the literature, but there is no standard protocol and no consistent response (17–20).

Our data are the first to describe the Hedgehog pathway as a potential new therapeutic target in both human MTC tissue by immunohistochemical staining and in two previously characterized and well-established MTC cell lines, one with an infamously aggressive RET mutation (M918T, MZ-CRC-1 cell line). Treatment of cell lines with SAG and GDC, agonists and antagonists of Smo respectively, demonstrated by mRNA and protein detection methods that the Hh pathway can be easily manipulated through the canonical signaling pathway. Our results also suggest that inhibition of Hh signaling reduces cell number and viability at least in part through apoptosis and activation of caspase-3 and -7. IHC staining in multiple samples of MTC shows variability in Hh staining pattern, similar to the variability previously reported in follicular thyroid tumors (9). Further studies are underway to determine whether Hh staining pattern is important in MTC clinical outcomes. Regardless, all MTC tumors sampled were positive for Hh activation by IHC methodology.

Aberrant Hh signaling has been previously described in multiple other tumors including basal-cell carcinoma, pancreatic cancer, colorectal cancer, hepatocellular carcinoma, medulloblastoma, and small-cell lung carcinoma (21–28). To date, aberrant upregulation of Hh signaling and proliferation of tumor cells can occur through mutations in downstream targets (e.g., PTCH1 mutations in Gorlin syndrome, sporadic basal-cell carcinoma) or, most commonly, through inappropriate expression of Hh ligand from the tumor with subsequent autocrine or paracrine signaling to the tumor cells or surrounding stromal tissue. Conversely, surrounding stromal cells have been described as producing Hh ligand that further stimulates tumor cell growth (27,28). It is yet unclear how Hh signaling interacts with mutagenic pathways in MTC. One recent *in vitro* study suggested that Gli1 upregulated wild-type RET expression in neural crest-derived ganglioneuromas, suggesting Hh may potentially interact with RET signaling (29). Future *in vivo* and immunohistochemical studies will be needed to examine this further in MTC.

GDC-0449, also known as vismodegib, is currently FDA approved for treatment of another ectodermally derived tumor, metastatic basal-cell carcinoma. In mutation-driven

tumors such as locally advanced or metastatic BCC and Gorlin syndrome, GDC-0449 has shown substantial tumor regression (30,31). One recent clinical trial enrolled 33 patients with distant metastatic basal-cell carcinoma and treated them with 150 mg of oral vismodegib daily (32). The trial reported an overall response rate of 30% ([CI 31–56%],  $p < 0.001$ ) among those with distant metastases and, impressively, reported complete responses in 13 patients (21%). In addition, 43% of patients with locally advanced BCC ([CI 30–56%],  $p < 0.001$ ) had a response with 24% of patients with locally advanced disease obtaining complete responses. Side effects from this drug included muscle spasms, dysgeusia, alopecia, fatigue, and weight loss. Of the 104 patients, only 13 (12%) had an adverse event that led to discontinuation of the study drug (32).

Our study is the first to describe Hh signaling in MTC with potential implications for novel therapy. Limitations of the study include all disadvantages of working with cell lines *in vitro*, including potential for morphogenesis and altered behavior in cell culture compared to behavior *in vivo*. Future animal and human studies will likely significantly contribute to our understanding of Hh signaling in MTC.

In conclusion, inhibition of the Hh pathway is a potential new therapeutic intervention for metastatic MTC. Further clinical studies should be performed to determine *in vivo* utility of the drug in patients with persistent disease after thyroidectomy.

#### Acknowledgments

We would like to acknowledge the Duke University Hospital T32 Endocrinology, Diabetes, and Nutrition Training Grant (2 T32 DK 007012-34), the Duke University Hospital Gastroenterology Divisional Research Funds, and R01 DK-077794 for support of this work.

#### Author Disclosure Statement

No competing financial interests exist.

#### References

- Valle LA, Kloos RT 2011 The prevalence of occult medullary thyroid carcinoma at autopsy. *J Clin Endocrinol Metab* **96**:E109–113.
- Marini F, Falchetti A, Del Monte F, et al. 2006 Multiple endocrine neoplasia type 2. *Orphanet J Rare Dis* **1**:45.
- Jimenez C, Hu MI, Gagel RF 2008 Management of medullary thyroid carcinoma. *Endocrinol Metab Clin North Am* **37**: 481–496, x–xi.
- Jeong J, Mao J, Tenzen T, et al. 2004 Hedgehog signaling in the neural crest cells regulates the patterning and growth of facial primordia. *Genes Dev* **18**:937–951.
- Ahlgren SC, Thakur V, Bronner-Fraser M 2002 Sonic Hedgehog rescues cranial neural crest from cell death induced by ethanol exposure. *Proc Natl Acad Sci USA* **99**:10476–10481.
- Ahlgren SC, Bronner-Fraser M 1999 Inhibition of Sonic Hedgehog signaling *in vivo* results in craniofacial neural crest cell death. *Curr Biol* **9**:1304–1314.
- Berger CL, de Bustros A, Roos BA, et al. 1984 Human medullary thyroid carcinoma in culture provides a model relating growth dynamics, endocrine cell differentiation, and tumor progression. *J Clin Endocrinol Metab* **59**:338–343.
- Cooley LD, Elder FF, Knuth A et al. 1995 Cytogenetic characterization of three human and three rat medullary thyroid carcinoma cell lines. *Cancer Genet Cytogenet* **80**: 138–149.
- Xu X, Ding H, Rao G, et al. 2012 Activation of the Sonic Hedgehog pathway in thyroid neoplasms and its potential role in cell proliferation. *Endour Relat Cancer* **19**:167–179.
- Sicklick JK, Li YX, Choi SS, et al. 2005 Role for Hedgehog signaling in hepatic stellate cell activation and viability. *Lab Invest* **85**:1368–1380.
- Sippel R, Kunnimalaiyaan M, Chen H 2008 Current management of medullary thyroid cancer. *The Oncologist* **13**:539–547.
- Kodama Y, Asai N, Kawai K, et al. 2005 The RET proto-oncogene: a molecular therapeutic target in thyroid cancer. *Cancer Sci* **96**:143–148.
- Asai N, Jijiwa M, Enomoto A, et al. 2006 RET receptor signaling: dysfunction in thyroid cancer and Hirschsprung's disease. *Pathol Int* **56**:164–172.
- Wells SA Jr, Robinson BG, Gagel RF, et al. 2012 Vandetanib in patients with locally advanced or metastatic medullary thyroid cancer: a randomized, double blind phase III trial. *J Clin Oncol* **30**:134–141.
- Lanzi C, Cassinelli G, Nicolini V, et al. 2009 Targeting RET for thyroid cancer therapy. *Biochem Pharmacol* **77**:297–309.
- Romei C, Mariotti S, Fugazzola L, et al. 2010 Multiple endocrine neoplasia type 2 syndromes (MEN2): results from the ItAMEN network analysis on the prevalence of different genotypes and phenotypes. *Eur J Endocrinol* **163**:301–308.
- Shimaoka K, Schoenfeld DA, DeWys WD, et al. 1985 A randomized trial of doxorubicin versus doxorubicin plus cisplatin in patients with advanced thyroid carcinoma. *Cancer* **56**:2155–2160.
- De Besi P, Busnardo B, Toso S, et al. 1991 Combined chemotherapy with bleomycin, adriamycin, and platinum in advanced thyroid cancer. *J Endocrinol Invest* **14**:475–480.
- Wu LT, Averbuch SD, Ball DW, et al. 1994 Treatment of advanced medullary thyroid carcinoma with a combination of cyclophosphamide, vincristine, and dacarbazine. *Cancer* **73**:432–436.
- Orlandi F, Caraci P, Berruti A, et al. 1994 Chemotherapy with dacarbazine and 5-fluorouracil in advanced medullary thyroid cancer. *Ann Oncol* **5**:763–765.
- Scales SJ, de Sauvage FJ 2009 Mechanisms of Hedgehog pathway activation in cancer and implications for therapy. *Trends Pharmacol Sci* **30**:303–312.
- Johnson RL, Rothman AL, Xie J, et al. 1996 Human homolog of patched, a candidate gene for the basal cell nevus syndrome. *Science* **272**:1668–1671.
- Pietsch T, Waha A, Koch A, et al. 1997 Medulloblastomas of the desmoplastic variant carry mutations of the human homologue of *Drosophila* patched. *Cancer Res* **57**:2085–2088.
- Raffel C, Jenkins RB, Frederick L, et al. 1997 Sporadic medulloblastomas contain PTCH mutations. *Cancer Res* **57**: 842–845.
- Vorechovsky I, Tingby O, Hartman M, et al. 1997 Somatic mutations in the human homologue of *Drosophila* patched in primitive neuroectodermal tumours. *Oncogene* **15**:361–366.
- Fan L, Pepicelli CV, Dibble CC, et al. 2004 Hedgehog signaling promotes prostate xenograft tumor growth. *Endocrinology* **145**:3961–3970.
- Dierks C, Grbic J, Zirlik K, et al. 2007 Essential role of stromally induced Hedgehog signaling in B-cell malignancies. *Nat Med* **13**:944–951.

28. Yauch RL, Gould SE, Scales SJ, et al. 2008 A paracrine requirement for Hedgehog signaling in cancer. *Nature* **455**:406–410.
29. Gershon TR, Shirazi A, Qin LX et al. 2009 Enteric neural crest differentiation in ganglioneuromas implicates Hedgehog signaling in peripheral neuroblastic tumor pathogenesis. *PloS One* **4**:e7491.
30. Von Hoff DD, LoRusso PM, Rudin CM, et al. 2009 Inhibition of the Hedgehog pathway in advanced basal-cell carcinoma. *N Engl J Med* **361**:1164–1172.
31. Tang JY, Mackay-Wiggan JM, Aszterbaum M, et al. 2012 Inhibiting the Hedgehog pathway in patients with the basal-cell nevus syndrome. *N Engl J Med* **366**:2180–2188.
32. Sekulic A, Migden MR, Oro AE, et al. 2012 Efficacy and safety of vismodegib in advanced basal-cell carcinoma. *N Engl J Med* **366**:2171–2179.

Address correspondence to:

*Brittany N. Bohinc, MD*

*310 Baker House*

*210 Trent Drive*

*Durham, NC 27710*

*E-mail: brittany.bohinc@duke.edu*